České vysoké učení technické v Praze
Fakulta jaderná a fyzikálně inženýrská

Czech Technical University in Prague
Faculty of Nuclear Sciences and Physical Engineering

doc. Dr. rer. nat. Jesús Guillermo Contreras Nuño

Fotoprodukce vektorových mezonů na LHC: prosvětlení vysokoenergetické kvantové chromodynamiky.

Photoproduction of vector mesons at the LHC: shining light into high-energy QCD

Summary

The high-energy limit of QCD is very interesting. In particular, it is expected that at some high energy the structure of hadrons changes from a dilute to a saturated state. The search for signals of the onset of saturation is one of the most active topics of research in QCD today.

One set of observables that offers a clean environment to search for saturation phenomena is provided by photon-induced processes. The advent of LHC data has rekindle both theoretical and experimental interest in this area.

In this Lecture, I review the most important experimental results from the ALICE Collaboration regarding the photoproduction of a vector meson, as well as the implication these data have had in our understanding of saturation, in particular in the development of new models that include quantum fluctuations on the QCD structure of hadrons in the impact parameter plane.

Souhrn

Vysokoenergetický limit kvantové chromodynamiky je velmi důležitý. Očekává se, že při určité energii struktura hadronů přejde od volného do saturovaného stavu. Hledání signálů nástupu saturace je jednou z hlavních otázek dnešního výzkumu kvantové chromodynamiky.

Jednou z možností, jak sledovat tento fenomén, jsou procesy indukované srážkou s fotony. Data z experimentu v LHC znovu zažehl zájem jak teoretické, tak i experimentální části fyzikální obce na tomto poli.

V této přednášce představím nejdůležitější experimentální výsledky kolaborace ALICE z pole fotoprodukce vektorových mezonů. Budu mluvit také o tom, jak nám tato data pomohla pochopit saturaci. Jmenovitě se budu zabývat vývojem nových modelů, které zahrnují kvantové fluktuace struktury hadronů v rovině příčné vzdálenosti.

Klíčová slova:

QCD, saturace, detektor ALICE, LHC

Key words:

QCD, Saturation, ALICE detector, LHC

Contents

1 Introduction

Quantum Chromodynamics, QCD, is a relativistic quantum field theory that attempts to describe one of the fundamental forces of nature, the strong interaction [1]. Its fields are quarks and gluons which are constituents of all hadrons — particles that feel the strong force.

The basic idea of QCD is to exploit the gauge symmetry of a group. This is also the basic idea of Quantum Electrodynamics, the only difference being the corresponding group. In QCD the group is SU(3), which is non-abelian. This group gives a great richness to QCD. There are three types of strong charges, known as colour charges and denoted as green, blue and red. The carriers of these charges are not only the quarks; in QCD also the gluons carry colour charge and hence can interact among themselves.

The interaction among quarks and gluons are balanced such that the force between a probe and a test charge increases with their separation. This leads to two phenomena known as confinement and asymptotic freedom. Confinement implies that there are no free colour charges at the current energies of our every day life, but that all colour charges are within bound objects which are colour neutral. These objects are the hadrons mentioned above and include, among many others, the protons, neutrons and all nuclei made out of them. Asymptotic freedom means that at short distances the colour charges can be considered as quasi-free, at least for very short periods of time, which opens the door to the application of perturbative techniques to solve QCD in this domain.

As all colour charges are confined inside hadrons and the basic hadrons are quite small it is very difficult to study QCD. But it is also very rewarding. The QCD structure of the proton was extensively studied at the HERA collider. The picture that emerged is that of a proton composed of quarks and gluons sharing each a given fraction (denoted by x) of the total four momentum of the proton and that the number of quarks and gluons seen by a probe depends on the energy of the interaction and the resolution of the probe [2]. This is illustrated in Fig. 1. It also

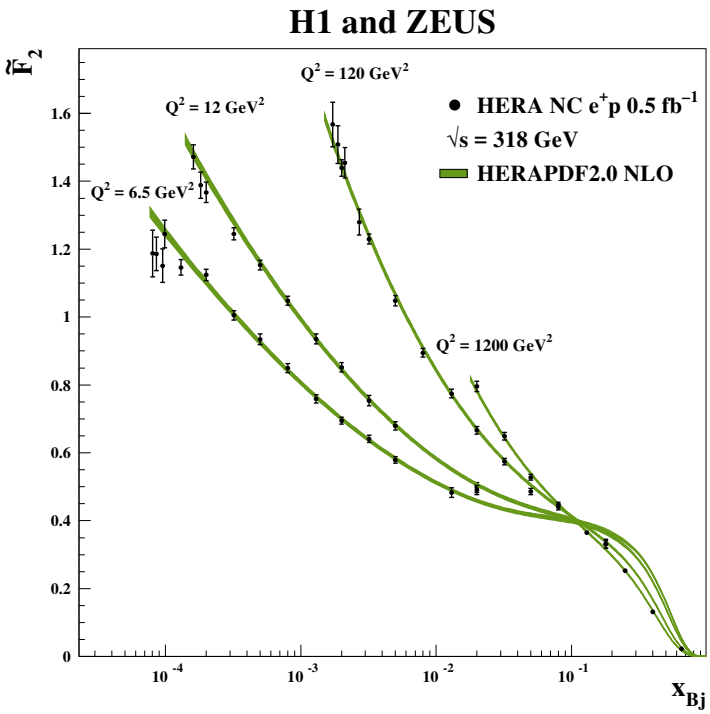

Figure 1: Structure function of the proton as a function of x (denoted by x_{Bj} in the axis) for different scales Q^2 of the interaction. Figure taken from [2].

emerged that at high energies, which correspond to small values of x, the proton structure is dominated by contributions of the gluon field and that the number of gluons in the proton grows rapidly with decreasing x (for large scales Q^2 — corresponding to very good resolution of the probe — which allows the use of perturbative QCD). This is illustrated in Fig. 2. It is expected that at some point the phase space of the proton fills with gluons and a new regime, called gluon saturation, sets in [3]. One of the most pressing questions nowadays in QCD is to find signals of

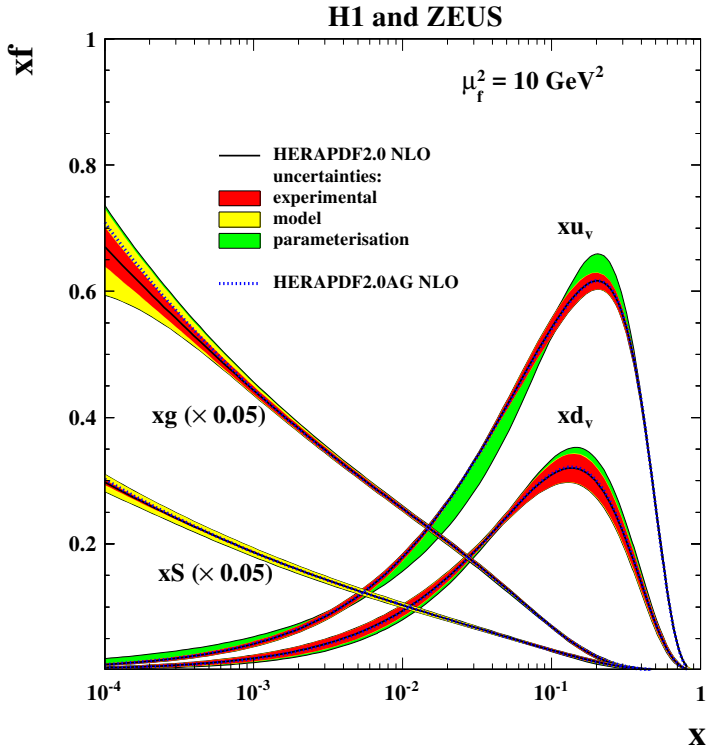

Figure 2: Parton density functions extracted from structure function data using perturbative QCD. Note that the gluon and sea-quark distributions have been scaled by a factor of 20. Figure taken from [2].

saturation.

Currently, the best place to search experimentally for these signals is the Large Hadron Collider (LHC) [4], where collisions of protons on protons, protons on lead ions and of lead ions are carried out at the largest energies ever reached in the laboratory. The LHC started operation at the end of 2009 and provided collisions until 2013, a period called the LHC Run 1. After improvements both to the accelerator and to the detectors — which

Table 1: Different collisions systems and the corresponding centre-of-mass energy $\sqrt{s}$ for the LHC during Run 1 (upper part) and Run 2 (lower part).

Year	System	$\sqrt{s}$ (TeV)
2009, 2010	pp	0.9
2011	pp	2.76
2010, 2011	pp	7
2012	pp	8
2013	pPb	5.02
2010, 2011	PbPb	2.76
2015	pp	5.02
2015–2016	pp	13
2016	pPb	5.02
2016	pPb	8.16
2015, 2018	PbPb	5.02
2017	XeXe	5.44
2018	pp	13

record the collisions — the LHC restarted operation in 2015 and will provide collisions until the end of 2018, a period called the LHC Run 2. With respect to Run 1, there is much more data from Run 2 and the data are being collected at a higher collision energies. See Tab. 1 for a brief overview of the collision systems provided by the LHC up to the end of Run 2.

Below we discuss some results obtained by the ALICE Collaboration. A group of some 1500 scientists, engineers and students from 37 countries that has designed and built a complex system of detectors called also ALICE [5]. ALICE is a very complex apparatus composed of some 20 different large subsystems, among them the V0 and the AD detectors, which have been designed, built and operated with a strong participation of both Cinvestav (Mex) and ČVUT (CZ), and which are key instruments for the measurements presented in the following sections.

2 The LγHC

As mentioned in the preceding section, the LHC accelerated protons and lead nuclei to very large energies. Both of these types of particles are electrically charged; as such carry with them an electromagnetic field. Long ago, Fermi suggested [6] that a strongly Lorentz-contracted electromagnetic field would look like a source of quasi-real photons.

For the conditions available at the LHC the virtuality of the quasi-real photons is very small — of the order of a few MeV — when the source are lead nuclei, because it is related to the transverse size of the emitting particle and lead ions are, in this context, big. On the other hand, the maximum energy of the photons in the laboratory frame is given by the boost of the fast particle. As at the LHC the same magnets are used to accelerate both protons and ions, the Lorentz factor is larger for the former. The maximum energies that the photons reach are of the order of 80 GeV and 2.4 TeV for photons emitted by lead or by protons, respectively [7]. The maximum centre-of-mass energy for photon–lead (γPb) and photon–proton (γp) interactions at the LHC reaches 1.5 TeV and 8.4 TeV, respectively [7].

The flux of photons depends on the square of the electric charge (Z) of the fast particle, making the lead ions ($Z = 82$) a copious source of photons at the LHC. The large flux of photons and the unprecedented energies that can be reached, convert the LHC into a LγHC and make it possible to study photoproduction processes in this facility.

One example of the processes we are interested in here is shown in Fig. 3. A nucleus in the incoming Pb beam emits a quasi-real photon which then interacts with a proton to create a vector meson. As a by-product of the interaction the proton may dissociate into a low-mass system. Similar (but not entirely equal) processes exist also for lead targets; these processes are called coherent and incoherent photonuclear production, respectively.

What makes these processes special is that the kinematics of the event is completely determined by measuring the produced

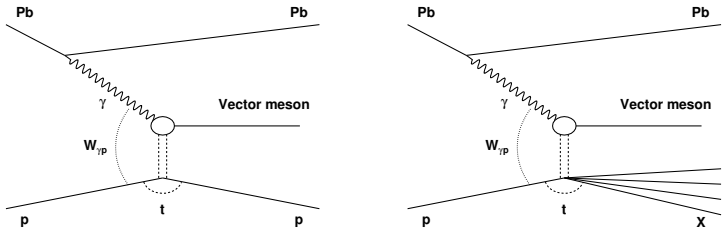

Figure 3: Diagrams for the exclusive (left) and dissociative (right) photoproduction of a vector meson off a proton at the LHC. A lead ion emits a quasi-real photon (upper vertex) which then interacts with the incoming proton to produced a vector meson. In the exclusive case the proton remains intact, while in the other case the proton dissociates into a low-mass state.

vector meson. Its transverse momentum allows one to determine the square of the momentum transferred at the proton vertex (t), while its scattering angle determines the centre-of-mass energy of the γp scattering ($W_{\gamma \mathrm{p}}$), which can be used to compute x.

As mentioned above, the structure of the proton depends on x and the resolution of the probe. Using different vector mesons allow us to change the scale of the resolution (which for photoproduction is given solely by the mass of the vector meson), while measuring the vector meson at different scattering angles allow us to cover a large range of x values, and in particular to search for saturation effects at the largest energies ever reached in the laboratory with these processes. A first review of results achieved in this field at the LHC was presented in [8].

3 ALICE and photoproduction of vector mesons

The processes shown in Fig. 3 have a very clean signature. In the detector one finds only the decay products of the vector meson; e.g. for a J/ψ a $\mu^+\mu^-$ or and e^+e^- pair. As there is only one particle produced and the incoming beams are aligned in

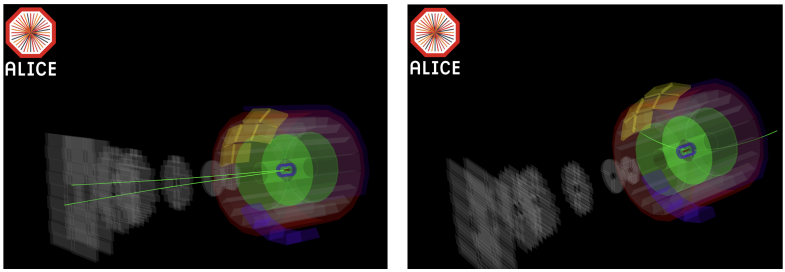

Figure 4: Displays of ALICE photoproduction events. These are candidates for the photonuclear production of a J/ψ decaying into two muons measured by the forward muon spectrometer (left) or an electron-positron pair measured in the central barrel.

the longitudinal direction, there is no transverse momentum and hence the vector meson has a very small transverse momentum (that allowed by the size of the incoming particles and the uncertainty principle, which for lead is some 30 MeV/c and for protons is some 250 MeV/c). So, the experimental strategy to look for these type of events is to measure a vector meson with very small transverse momentum and to make sure that there is nothing else in the detector. (For the dissociative case, one may find some activity in the very forward direction. In addition, due to the very strong electromagnetic field of lead ions, there may be some neutrons at beam rapidity produced by other independent electromagnetic interactions.)

ALICE [5, 9] has two main sections: the central barrel and the forward muon spectrometer. The decay products of the vector meson can be measured in any of these sections. Two examples can be seen in Fig 4. The detector depicted in gray and shown towards the left side of the event displays is the muon forward spectrometer. The rest of the detectors shown in Fig 4 form the central barrel of ALICE, which consists of the Inner Tracker System (ITS), the Time Projection Chamber (TPC) and the Time-of-Flight (TOF) detector. In order to make sure that there are no other particles in the event, and to tag the occurrence of disso-

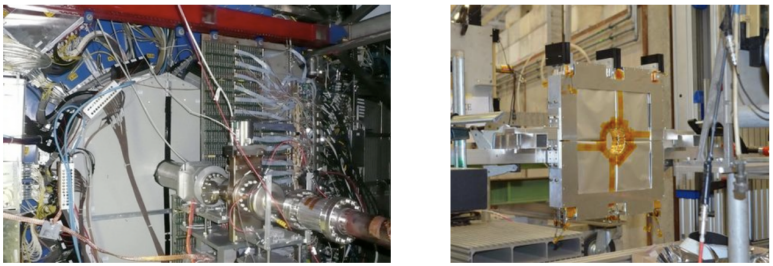

Figure 5: The V0-A detector (left) installed inside the ALICE detector system. The beam pipe is clearly seen as well as some of the read-out electronics and cables carrying the electric power to the different components. The AD detector (right) during a beam test.

ciative events, we use the V0 and the AD detectors. Photographs of these two detectors are shown in Fig. 5.

The V0 detector [10] consists of two arrays of plastic-scintillator detectors called V0-A and V0-C. The V0-A array was designed and built in Mexico, while the V0-C in France. Each array is segmented in four rings in the radial direction and 8 azimuthal sectors. The arrays use WLS fibres, which conduct the light, produced by particles traversing the plastic, to photomultiplier tubes (PMT). The signal from the PMT is split into two signals. One is amplified and used to obtain timing information with a TDC. The other is not amplified and it is used to obtain charge information with an ADC. The timing information can be used to trigger for the presence or absence of activity. The charge information can be used to trigger on the amount of activity in a given event.

The arrays are placed in opposite sides of the nominal interaction point and cover the pseudo-rapidity ranges (2.8,5.1) and (-3.7,-1.7) for the V0-A and V0-C, respectively. This large rapidity coverage is very useful for measurements of diffraction events [11] as well as for the study of the photoproduction processes discussed here.

The AD detector is similar to the V0 detector in philosophy

and construction. It is also made of scintillator plastic read out by optical fibres and PMTs. The electronics and data acquisition system are also similar to that from V0. The AD detector was integrated in ALICE during the LHC shutdown before Run 2 to enhance the capabilities of the experiment to tag diffractive processes and events with low transverse momentum. It consists of two double layers of scintillation counters placed far from the interaction region, on both sides: one in the ALICE cavern at 17.0 m and one in the LHC tunnel at -19.5 m. Its good time resolution and large coverage in pseudorapidity, extending up (down) to 6.3 (-7.0) units is very useful to tag the presence of inelastic collisions and to select events with large forward-rapidity gaps, like central diffraction production or exclusive photoproduction processes.

4 Photoproduction off nuclei

Before the start of the LHC, it was not clear if the type of processes depicted in Fig. 3 could be measured with competitive precision at the LHC. The largest detectors, ATLAS and CMS, were designed to study very hard processes, while ALICE was built to investigate events where thousands of particles are produced. Furthermore, electromagnetic radiation from the beams is hurtful for the LHC, which runs its magnets in a superconducting state and any additional heat may disturb their performance. In contrast, the study of photo-induced processes requires a large photon flux and detectors that can trigger and measure events with only very few, and very soft, particles. Nonetheless, a group was stablished in ALICE to study the feasibility of contributing to this field.

After successful tests of a trigger strategy using data from 2010, data from the 2011 Pb-Pb collision period was good enough, and the collected data set was large enough, to produce valuable scientific output. The first article from the LHC in this field was published by ALICE in 2013 [13]. It reported the measurement of J/ψ photoproduction off lead ions at forward rapidities. This

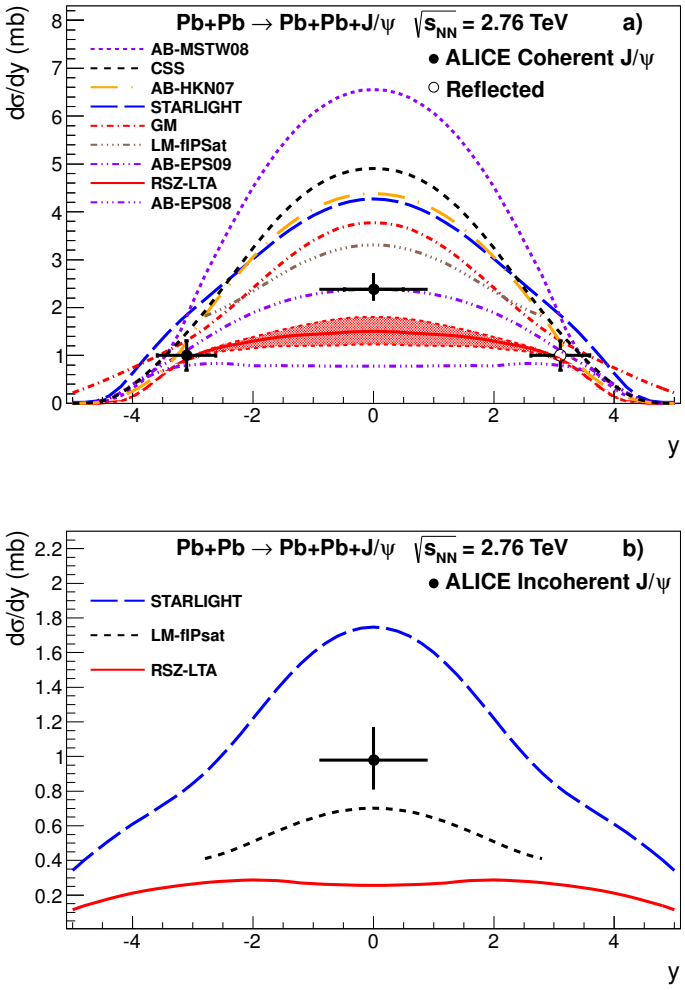

Figure 6: Cross section for coherent (upper panel) and incoherent (lower panel) photoproduction of a J/ψ off a lead nucleus as a function of rapidity measured by ALICE; the measurements are compared to several predictions. Figures taken from [12].

paper demonstrated not only the feasibility, but also the competitiveness of this type of measurements at the LHC and opened up a new field of study. Nowadays all four large collaborations at the LHC (ALICE, ATLAS, CMS and LHCb) have published results on photoproduction processes; the availability of new data has rekindled the interest of the theory and phenomenology communities, making that this field is very active nowadays.

This first article was followed soon by another one [12]. The main results of these two articles are shown in Fig. 6. The upper panel shows the coherent photonuclear production of J/ψ off a lead ion. The point at rapidity (y) $-3.6 < y < -2.6$ corresponds to the first measurement reported in [13]. The cross section in this case is dominated by relatively large values of $x \approx 0.01$. The second measurement at $-0.9 < y < 0.9$ corresponds to $x \approx 10^{-3}$. The figure clearly shows that the the predictions which were more or less close to each other and to data at large x spread out as x diminished. The measurement is sensitive to the amount of nuclear shadowing[1]. The best description is achieved by models incorporating a moderate amount of gluon shadowing and disfavours models with no shadowing at all or with very strong shadowing. Gluon saturation, if present, would contribute to shadowing at low x. The lower panel of Fig. 6 shows the incoherent photonuclear production of a J/ψ off a lead nucleus at mid-rapidity. The model closest to data is based on a prescription that includes saturation effects [14].

ALICE investigations continued with the measurement of the coherent cross section for the production of ρ^0 [17] and of ψ(2S) [18] off lead at mid-rapidity. The ρ^0 measurement is very interesting because the cross section is very large, with models predicting that it may reach 50% or more of the total inelastic cross section. This makes it possible that the black disk limit could be reached. Furthermore, the model description of the measured data (not only by ALICE, but also by STAR at RHIC) offered

[1]Shadowing is the experimental fact that the cross section for deep-inelastic scattering off nuclei at low x is smaller than the nucleon cross section multiplied by the atomic mass number of the nucelus.

some puzzles: a model [19] which does not include the elastic part of the total cross section describes best the data, while a model [20] which a priori includes all the contributions is a factor of two off the measurement. (See discussion in [17].) The ρ^0 measurement triggered new phenomenological studies to try to understand this situation; see, e.g. [21]. The measurement of ψ(2S) is important, because one of the main uncertainties in the modeling of this kind of processes is the wave function of the vector meson. Both the J/ψ and ψ(2S) have a similar mass, so the main difference is the wave function, which in the case of the ψ(2S) includes a node [22]. The results from ψ(2S) supported the conclusions reached by the J/ψ measurements.

The previous results were obtained in so called ultra-peripheral collisions (see e.g. [8]) where the incoming nuclei are separated by an impact parameter larger than the sum of their radii. Unexpectedly, ALICE discovered that coherent photoproduction of J/ψ was also visible in peripheral collisions where the incoming nuclei also interact purely hadronically [15]. The left panel of Fig. 7 shows the nuclear suppression factor[2] ($R_{\rm AA}$) for J/ψ production as a function of centrality in three different ranges of the J/ψ transverse momentum. $R_{\rm AA}$ is expected to be below one for inelastic collisions due to gluon shadowing and to approach one for very peripheral events. This is seen for the two larger transverse-momentum ranges. But the measurement at the lowest transverse momentum shows a huge increase for peripheral events with $R_{\rm AA}$ reaching values up to 7. The only feasible explanation of this behaviour is that there is a contribution from photonuclear production of J/ψ which causes the increment in $R_{\rm AA}$.

This result is very important for several reasons. One of them, relevant for the topic discuss here, is that, in conjunction with the results of ultra-peripheral collisions [13] it allow us to extract the γPb cross section out of the Pb–Pb cross section. This was

[2]The nuclear suppression factor is computed as the ratio of the nuclear cross section for a given process, divided by the nucleon cross section for the same process scaled by the nuclear overlap function.

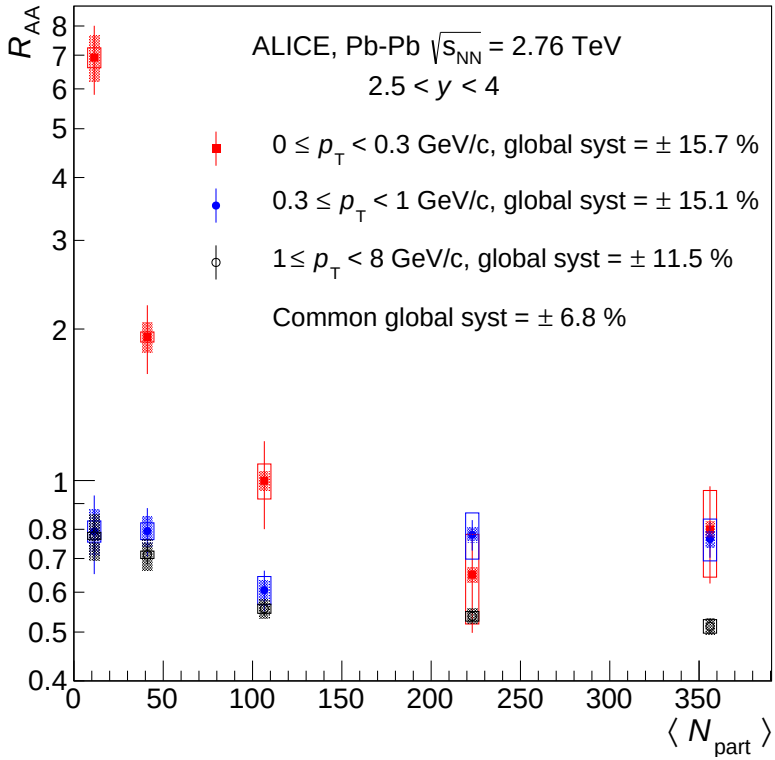

Figure 7: Nuclear suppression factor, $R_{\rm AA}$, for J/ψ production in Pb–Pb collisions as a function of centrality for three different ranges of J/ψ transverse momentum. The lowest range shows a surprising increase, well beyond one, for peripheral centralities. Figure taken from [15].

achieved in [16] and it is shown in the right panel of Fig. 7. ALICE measurements allow us to reach x values as low as 5×10^{-5}, which is almost two orders of magnitude lower than what was previously achieved. Furthermore, the cross section at the lowest x-value seems to be below than a power law extrapolation of the two measurements at higher x values.

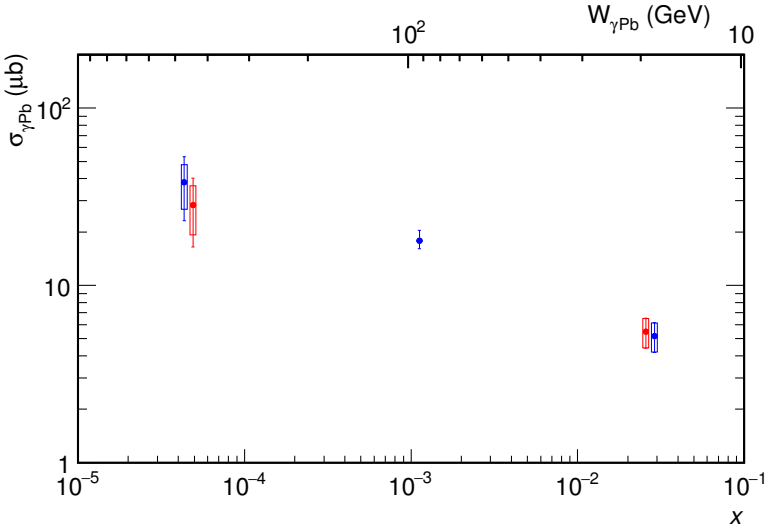

Figure 8: Photonuclear coherent production of J/ψ as a function of x (or the photon–Pb centre-of-mass energy) as extracted from ALICE data. Figure taken from [16].

5 Photoproduction off protons

The ideal system to study photoproduction of vector mesons off protons at the LHC is that provided by proton-lead collisions. As mentioned before, the intensity of the photon flux is much larger for Pb than for p which guarantees that most of the photon induced processes are of the γp type.

ALICE studied the energy dependence of exclusive J/ψ photoproduction [23] using the forward muon spectrometer, which allowed ALICE to access either small or large centre-of-mass energies of the γp system. This is so, because the LHC switched the direction of both beams at the middle of the data taking period. Collisions where the proton beam was travelling toward (away from) the spectrometer corresponded to low (large) energies, or equivalently to large (small) values of x.

The results are shown in Fig. 9 and compared to data from

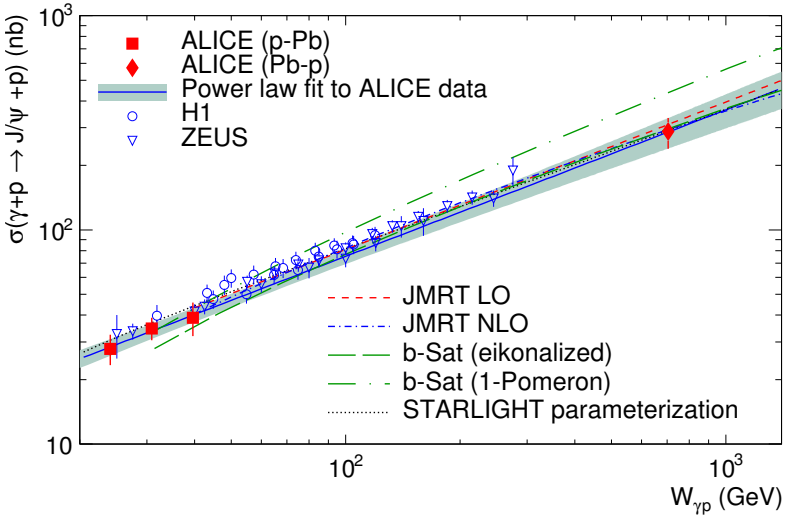

Figure 9: Exclusive photoproduction of J/ψ off a proton as a function of the centre-of-mass energy of the photon-proton system. Data from ALICE (red) are compared to previous data from HERA (blue) and to model predictions (lines). A power law fit (band) to ALICE data is also shown. Figure taken from [23].

HERA, model predictions and a power law fit to ALICE data. At low energies ALICE and HERA data agree. At high energies, ALICE managed to reach more than twice the largest energy accessible at HERA. This is a remarkable achievement. All models, except b-Sat (eikonalised), as well as the fit, describe correctly the data. The signature for saturation would be a departure from the power law behaviour at large energies, such that the trend flattens out and becomes less steep as energy increases. With the precision of data from [23] no signal of saturation has been seen, although models incorporating saturation describe correctly the data, which is also well describe by models without saturation effects.

There are two possible improvements to this measurement. A better coverage of the phase space so that the power law fit

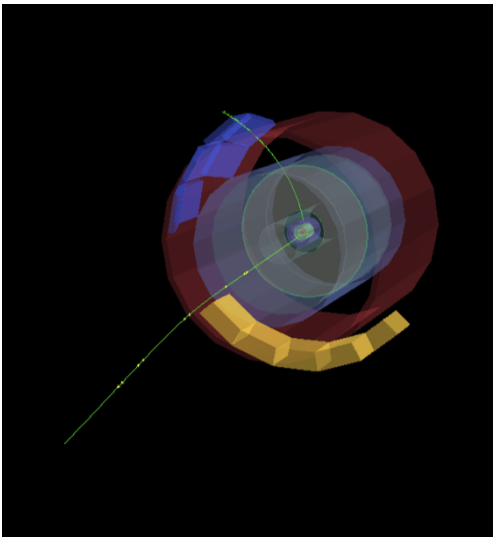

Figure 10: ALICE event display for a J/ψ candidate decaying into a $\mu^+\mu^-$ pair where on of the muons is measured in the central barrel and the other in the forward muon spectrometer. This topology allows us to measure J/ψ production in rapidity ranges which have no instrumentation in ALICE.

is better constrained and an increase in the energy reach. To address the first aspect ALICE measured the photoproduction of J/ψ using another two configurations. One where the decay products of the J/ψ are measured in the central barrel (see Fig. 4, right) and a novel configuration where one muon is measured in the central barrel and the other in the forward muon spectrometer. This new topology allows us to measure J/ψ at rapidities where ALICE has no instrumentation. An event display of such a candidate is shown in Fig. 10. Figure 11 shows preliminary measurements of the energy dependence of the cross section for J/ψ photoproduction off protons.

The second potential improvement mentioned above is an increase on the energy reach. The measurements just described were obtained from p–Pb collisions at a centre-of-mass energy of

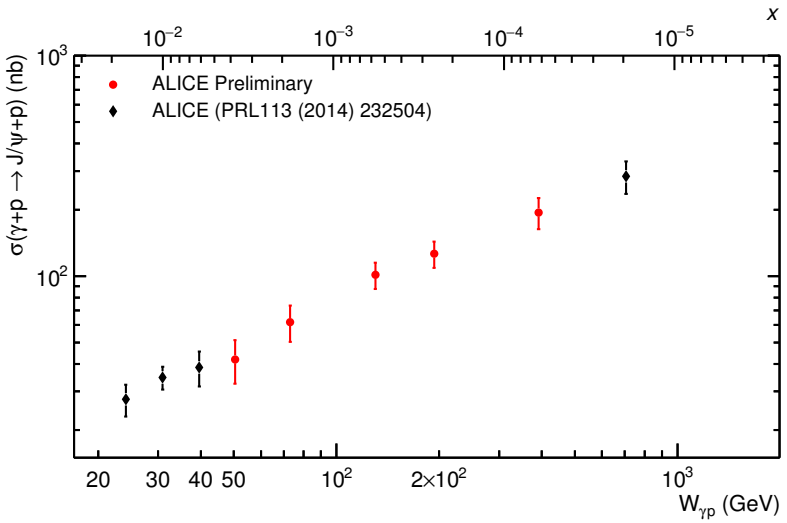

Figure 11: Energy dependence of J/ψ photoproduction off protons. The data shown with black markers were published in [23]. The two points shown with red markers at the lowest energy, as well as the red point shown at the highest energy, are cross sections measured using the topology shown in Fig. 10. The remaining two measurements shown with red markers were performed using events with the decay products of the J/ψ measured in the central barrel of ALICE, as for example shown in the event display of Fig. 4.

5.02 TeV. During 2016 ALICE collected new data at an energy of 8.16 TeV (see Tab. 1). Furthermore, the AD detector was active and taking part in the trigger during this period. This will allow ALICE to perform measurements, which will reach centre-of-mass energies up to 1.5 TeV for the γp system. The analysis of these data will open up new possibilities in the search for saturation effects.

6 Geometrical fluctuations in the transverse structure of hadrons

The advent of the LHC data, which combine the possibility to cross check with HERA results with a huge increase in the maximum energy that can be reached has rekindle interest in phenomenological studies of these processes in the context of the high-energy limit of perturbative QCD. One of the developments has been the appearance of models considering the geometrical distribution of gluons within the incoming proton. Models of this type based on the Good-Walker approach [24, 25] described the exclusive process as an average over the different configurations of the target, while the dissociative process is proportional to the variance over configurations.

In the particular model presented in [26] the gluon field of the proton is described as a set of hot spots (regions of high-gluon density) distributed randomly in the impact parameter plane of the highly contracted proton participating in interactions like those depicted in Fig. 3. The key ingredient of the model is that the number of these hot spots increases with decreasing x. This is depicted in Fig. 12. When the number of hot spots in the proton is large, then it fills up and the variance over configurations decreases signaling that all configurations look the same. This phenomenon is reminiscent of percolation. The original model was presented for J/ψ as the produced vector meson. The model was later on extended to cover nuclear targets [27] as well as other vector mesons [28].

A summary of the main results for photoproduction of a vector meson off a proton is shown in Fig. 13. The cross section for the exclusive production process shows different slopes depending on the mass of the vector meson and describes correctly the behaviour seen in data. For the dissociative process there is less data and their precision is worse. Nonetheless the model describes correctly the behaviour of data where available, as shown in Fig. 14.

The most remarkable prediction of the model concerns the be-

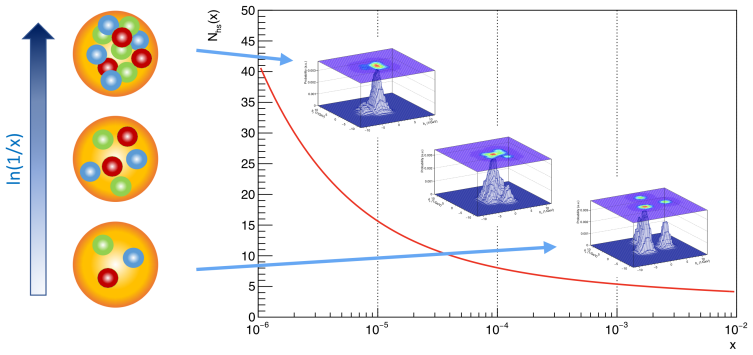

Figure 12: Schematic representation of the energy dependence of the hot-spot model presented in [26]. At large values of x the proton is described with three hot spots each of them described by a Gaussian density in the impact parameter plane (lower 'proton' on the left and first lego plot on the right). As the energy increases, or equivalently x decreases, more hot spots appear inside of the proton, while keeping the total probability of finding a hot spot constant. For a large number of hot spots (upper 'proton' on the left and corresponding lego plot) the proton saturates and all configurations are similar.

haviour of the dissociative cross section. As soon as the number of hot spots is large enough, the cross section reaches a maximum and afterwards decreases steeply towards higher energies. The position of the maximum depends on the mass of the vector meson: it is at larger energies for heavier vector mesons. The strength of this prediction is two fold. First, the predicted behaviour is a lot easier to spot than for the case of the exclusive production; second, the energy range where such a behaviour is expected is, according to the model, within the capabilities of existing HERA data (for the ρ^0) and of current and future LHC data (for all vector mesons depicted in Fig. 14).

The measurement of the energy dependence of the dissocia-

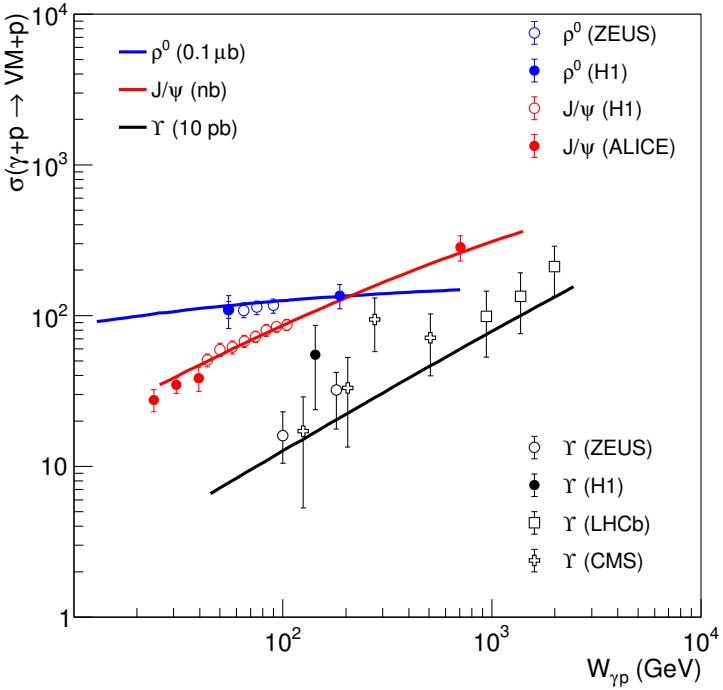

Figure 13: Exclusive production of a vector meson off a proton as a function the centre-of-mass energy of the γp system for different vector mesons. The model predictions (lines) are compared with the available data from HERA and the LHC. Figure taken from [28].

tive production of vector mesons is currently on of the goals of ALICE, where the low-mass dissociated system coming from the proton can be efficiently tagged using the AD detector.

7 Summary and outlook

The high-energy limit of perturbative QCD is a very active topic of research nowadays. In particular, the search for saturation

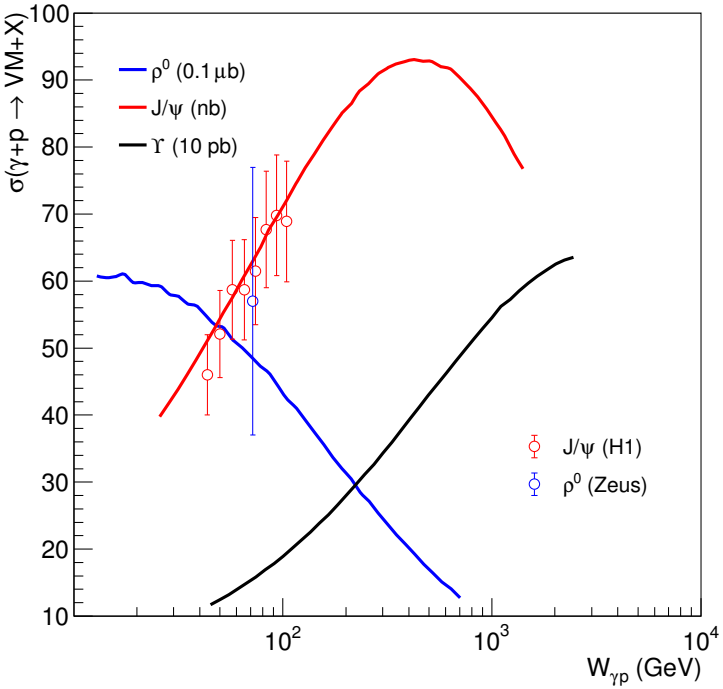

Figure 14: Dissociative production of a vector meson off a proton as a function the centre-of-mass energy of the γp system for different vector mesons. The model predictions (lines) are compared with the available data from HERA. Figure taken from [28].

and signals thereof has generated a large body of research, both theoretical and phenomenological, as well as experimental. One of the cleanest probes of the dynamical evolution of the QCD structure of hadrons is provided by the photoproduction of a vector meson off a hadronic target.

With the advent of LHC data from Run1 this area got a new impetus and is currently a very fertile field. From the experimental side, new results are eagerly expected from the Run 2 LHC data which has already been taken and from the data to

be collected towards the end of 2018, where the largest sample of Pb–Pb collisions at a centre-of-mass energy of 5.02 TeV is expected.

Afterwards the LHC and its detectors will enter two years of upgrades and improvements to prepare them for the Run 3 data taking period, which is expected to take place from 2021 to 2023. For ALICE, and in particular for the group working on photon-induced processes, data from Run 3 will represent a huge increase on statistics. ALICE will shift from working as a triggered detector to a continuous read-out modus of operation. For analyses using data from Pb–Pb collisions the expected increase is from a few hundred events per measured cross section using Run 2 data to some hundred thousand of events in the central barrel and several tens of thousand events at forward rapidity. This huge increase in statistics will allow us to perform detailed multidimensional measurements and to reduce the systematic uncertainties dramatically, which may open the door to an experimental measurement of saturation effects.

References

[1] T. Muta, *Foundations of Quantum Chromodynamics: An Introduction to Perturbative Methods in Gauge Theories, (3rd ed.)*, vol. 78 of *World scientific Lecture Notes in Physics*. World Scientific, Hackensack, N.J., 2010.

[2] **ZEUS, H1** Collaboration, H. Abramowicz et al., *Combination of measurements of inclusive deep inelastic $e^{\pm}p$ scattering cross sections and QCD analysis of HERA data*, *Eur. Phys. J.* **C75** (2015), no. 12 580, [arXiv:1506.0604].

[3] L. V. Gribov, E. M. Levin, and M. G. Ryskin, *Semihard Processes in QCD*, *Phys. Rept.* **100** (1983) 1–150.

[4] L. Evans and P. Bryant, *LHC Machine*, *JINST* **3** (2008) S08001.

[5] **ALICE** Collaboration, K. Aamodt et al., *The ALICE experiment at the CERN LHC*, *JINST* **3** (2008) S08002.

[6] E. Fermi, *On the Theory of the impact between atoms and electrically charged particles*, *Z.Phys.* **29** (1924) 315–327.

[7] A. J. Baltz, *The Physics of Ultraperipheral Collisions at the LHC*, *Phys. Rept.* **458** (2008) 1–171, [arXiv:0706.3356].

[8] J. G. Contreras and J. D. Tapia Takaki, *Ultra-peripheral heavy-ion collisions at the LHC*, *Int. J. Mod. Phys.* **A30** (2015) 1542012.

[9] **ALICE** Collaboration, B. B. Abelev et al., *Performance of the ALICE Experiment at the CERN LHC*, *Int. J. Mod. Phys.* **A29** (2014) 1430044, [arXiv:1402.4476].

[10] **ALICE** Collaboration, E. Abbas et al., *Performance of the ALICE VZERO system*, *JINST* **8** (2013) P10016, [arXiv:1306.3130].

[11] **ALICE** Collaboration, B. Abelev et al., *Measurement of inelastic, single- and double-diffraction cross sections in proton–proton collisions at the LHC with ALICE*, *Eur. Phys. J.* **C73** (2013), no. 6 2456, [arXiv:1208.4968].

[12] **ALICE** Collaboration, E. Abbas et al., *Charmonium and e^+e^- pair photoproduction at mid-rapidity in ultra-peripheral Pb-Pb collisions at $\sqrt{s_{\rm NN}}$=2.76 TeV*, *Eur. Phys. J.* **C73** (2013), no. 11 2617, [arXiv:1305.1467].

[13] **ALICE** Collaboration, B. Abelev et al., *Coherent J/ψ photoproduction in ultra-peripheral Pb-Pb collisions at $\sqrt{s_{NN}} = 2.76$ TeV*, *Phys. Lett.* **B718** (2013) 1273–1283, [arXiv:1209.3715].

[14] T. Lappi and H. Mantysaari, *Incoherent diffractive J/Psi-production in high energy nuclear DIS*, *Phys. Rev.* **C83** (2011) 065202, [arXiv:1011.1988].

[15] **ALICE** Collaboration, J. Adam et al., *Measurement of an excess in the yield of J/ψ at very low $p_{\rm T}$ in Pb-Pb collisions at $\sqrt{s_{\rm NN}}$ = 2.76 TeV*, *Phys. Rev. Lett.* **116** (2016), no. 22 222301, [arXiv:1509.0880].

[16] J. G. Contreras, *Small x gluon shadowing from LHC data on coherent J/ψ photoproduction*, *Phys. Rev.* **C96** (2017), no. 1 015203, [arXiv:1610.0335].

[17] **ALICE** Collaboration, J. Adam et al., *Coherent ρ^0 photoproduction in ultra-peripheral Pb-Pb collisions at $\sqrt{s_{\rm NN}} = 2.76$ TeV*, *JHEP* **09** (2015) 095, [arXiv:1503.0917].

[18] **ALICE** Collaboration, J. Adam et al., *Coherent ψ(2S) photo-production in ultra-peripheral Pb Pb collisions at $\sqrt{s}_{\rm NN}$ = 2.76 TeV*, *Phys. Lett.* **B751** (2015) 358–370, [arXiv:1508.0507].

[19] S. R. Klein and J. Nystrand, *Exclusive vector meson production in relativistic heavy ion collisions*, *Phys. Rev.* **C60** (1999) 014903, [hep-ph/9902259].

[20] V. Rebyakova, M. Strikman, and M. Zhalov, *Coherent ρ and J/ψ photoproduction in ultraperipheral processes with electromagnetic dissociation of heavy ions at RHIC and LHC*, *Phys. Lett.* **B710** (2012) 647–653, [arXiv:1109.0737].

[21] L. Frankfurt, V. Guzey, M. Strikman, and M. Zhalov, *Nuclear shadowing in photoproduction of ρ mesons in ultraperipheral nucleus collisions at RHIC and the LHC*, *Phys. Lett.* **B752** (2016) 51–58, [arXiv:1506.0715].

[22] J. Nemchik, N. N. Nikolaev, E. Predazzi, and B. G. Zakharov, *Color dipole phenomenology of diffractive electroproduction of light vector mesons at HERA*, *Z. Phys.* **C75** (1997) 71–87, [hep-ph/9605231].

[23] **ALICE** Collaboration, B. B. Abelev et al., *Exclusive* J/ψ *photoproduction off protons in ultra-peripheral p-Pb collisions at* $\sqrt{s_{\rm NN}} = 5.02$ *TeV*, *Phys. Rev. Lett.* **113** (2014), no. 23 232504, [arXiv:1406.7819].

[24] M. L. Good and W. D. Walker, *Diffraction disssociation of beam particles*, *Phys. Rev.* **120** (1960) 1857–1860.

[25] H. I. Miettinen and J. Pumplin, *Diffraction Scattering and the Parton Structure of Hadrons*, *Phys. Rev.* **D18** (1978) 1696.

[26] J. Cepila, J. G. Contreras, and J. D. Tapia Takaki, *Energy dependence of dissociative* J/ψ *photoproduction as a signature of gluon saturation at the LHC*, *Phys. Lett.* **B766** (2017) 186–191, [arXiv:1608.0755].

[27] J. Cepila, J. G. Contreras, and M. Krelina, *Coherent and incoherent* J/ψ *photonuclear production in an*

energy-dependent hot-spot model, *Phys. Rev.* **C97** (2018), no. 2 024901, [arXiv:1711.0185].

[28] J. Cepila, J. G. Contreras, M. Krelina, and J. D. Tapia Takaki, *Mass dependence of vector meson photoproduction off protons and nuclei within the energy-dependent hot-spot model*, *Nucl. Phys.* **B934** (2018) 330–340, [arXiv:1804.0550].

doc. Dr. rer. nat. Jesús Guillermo Contreras Nuño

Born: 27.04.1967 Monterrey, Nuevo León; México

Professional experience

- Professor, Applied Physics Department, Cinvestav Merida, Mexico. From 1998 to 2016. (On leave of absence from 2012 to 2016.)
- Scientific associate, CERN, 2005.
- KF-FJFI-CVUT 2012 to date (Invited professor through Navrat project LK11209 from 2012 to 2016.)

Research interests

- Experiment: DIS, Relativistic heavy ion collisions.
- Phenomenology: High energy limit of QCD.

Thesis supervised

- Ph. D.: 10 finished, 3 in process.
- M. Sc.: 11 finished, 2 in process.
- B. Sc.: 14 finished.

Scientific production

- Articles outside big collaborations: 18 (including reviews).
- Articles with the H1 Collaboration: 214.
- Articles with the ALICE Collaboration: 207.
- Books edited: 5 (conference proceedings).
- Outreach articles: 24.
- Presentations in international conferences: more than 40.
- Conferences organised: 9 (as Chair or co-Chair).

Scientific leadership

- Member of the IHEPCCC panel of ICFA (2007-2008).
- Vice-President (2008-2009) and President (2009-2011) of the Particles and Fields Division of the Mexican Physics Society.
- Member of executive committee of the Mexican Network on High Energy Physics (2008-2010).
- Member of the executive committee of the H1 Collaboration (2009-2011).
- Convener of the UPC and Diffraction Section of the European Network Sapore Gravis (2012-2014).
- Convener of the UD group of the ALICE Collaboration (2014-2016, 2018-2020).
- Member of the Physics Board of the ALICE Collaboration (2014-2016, 2018-2020).
- Convener of the Luminosity group of the ALICE Collaboration (2016 to date)

Honours and recognitions

- Member of the Mexican Academy of Science (since 1998).
- Best Mexican young scientist in Exact Science 2005. (Award presented by the President of Mexico).
- Level III (highest) of the Mexican System of Researchers (since 2009).